Characterization of Heat Transfer Along a Silicon Nanowire Using Thermoreflectance Technique

Yan Zhang, James Christofferson, Ali Shakouri, Deyu Li, Arun Majumdar, Yiying Wu, Rong Fan, and Peidong Yang

***Abstract*—We studied heat transfer along a silicon nanowire suspended between two thin-film heaters using a thermoreflectance imaging technique. The thermoreflectance imaging system achieved submicrometer spatial resolution and 0.1 °C temperature resolution using visible light. The temperature difference across the nanowire was measured, and then its thermal resistance was calculated. Knowing the dimension of the nanowire (115 nm in width and 3.9 μm in length), we calculated the thermal conductivity of the sample, which is 46 W/mK. Thermal conductivity decreases with decreasing wire size. For a 115-nm-wide silicon nanowire, the thermal conductivity is only one-third of the bulk value. In addition, the transient response of the thin-film heaters was also examined using three-dimensional thermal models by the ANSYS program. The simulated thermal map matches well with the experimental thermoreflectance results.**

***Index Terms*—Heat transfer, Si nanowire, thermal conductivity, thermoreflectance.**

NOMENCLATURE

PTR	Platinum thermometer resistance.
$C_{\rm th}$	Thermoreflectance coefficient.
$Q_{\rm active}$	Heat power on active PTR.
$Q_{\rm inactive}$	Heat power on inactive PTR.
I	Current supplied to PTR.
V	Voltage measured across the PTR.
G_l	Thermal conductance.
$R_{\rm th}$	Thermal resistance.
d	Wire length.
A	Wire cross-sectional area.
β	Thermal conductivity.
ΔT_h	Temperature increase on active PTR.
ΔT_s	Temperature increase on inactive PTR.
C_v	Lattice heat capacity.
υ	Velocity of the sound in the material.
l	Mean free path.

Manuscript received April 12, 2004; revised September 29, 2005. This work was supported by the National Science Foundation under the Nanoscale Interdisciplinary Research Teams Program.

Y. Zhang, J. Christofferson, and A. Shakouri are with the Electrical Engineering Department, University of California at Santa Cruz, Santa Cruz, CA 95064 USA.

D. Li is with the Department of Mechanical Engineering, Vanderbilt University, Nashville, TN 37203 USA.

A. Majumdar is with the Mechanical Engineering Department, University of California at Berkeley, Berkeley, CA 94720 USA.

Y. Wu was with the Chemistry Department, University of California at Berkeley, Berkeley, CA 94720 USA. He is now with the Department of Chemistry, The Ohio State University, Columbus, OH 43210 USA.

R. Fan and P. Yang are with the Chemistry Department, University of California at Berkeley, Berkeley, CA 94720 USA.

Digital Object Identifier 10.1109/TNANO.2005.861769

I. INTRODUCTION

INNOVATIVE thermoelectric applications by utilizing low-dimensional structures, e.g., nanowire, have received a great deal of attention since Hicks and Dresselhaus first proposing that low-dimensional semiconductor structures could enhance thermoelectric properties in 1993 [1], [2]. It was believed that the low-dimensional structures could overcome the efficiency barriers imposed by the conventional bulk materials [3]–[5].

The thermoelectric properties of nanowires can be modified due to quantum confinement, sharp features of one-dimensional (1-D) density of energy states [2], [6], increased boundary scattering of electrons and phonons [7], [8], and modified electron–phonon and phonon–phonon scattering, etc. Understanding the distinct modifications in nanowire properties due to two-dimensional (2-D) quantum confinement is of critical importance in order to apply these nanowires to nanoelectronics, biomedical, photonics, and efficient energy conversion devices.

In thermoelectric applications, most attention has been focused on Bismuth and Bi_2Te_3 nanowires because they are traditionally considered as the most efficient thermoelectric materials at room temperature today [9]–[12]. Theoretical simulations have shown an order of magnitude improvement in thermoelectric figure-of-merit ZT for Bismuth nanowires as compared with bulk materials [13].

However, less attention has been directed to thermal properties of silicon and related materials' nanostructures. Recently Si/SiGeC and Si/SiGe superlattice microcoolers were demonstrated with a maximum cooling of 7 °C at a 100 °C stage temperature and a cooling power density of 600 W/cm^2 [14]–[16]. It is believed a nanowire structure with 2-D confinement as compared with the 1-D confinement in a superlattice could enhance its thermal properties even further. Theoretical calculations based on Callaway–Holland models [17] showed the thermal conductivity of a silicon nanowire decreases with reduced wire width. For example, thermal conductivity of 100-nm nanowires will be three times less than that of bulk material [18]. However, measurements of thermal properties on such small dimensions are extremely difficult to handle. To understand the underlying physics and verify the theoretical predictions, it is important to develop a reliable technique to measure the thermal properties of these nanowires. In terms of materials, silicon is the most common semiconductor material, thus if we could also improve its thermoelectric properties by engineering its band structure utilizing low-dimensional confinement, this would be an ideal and innovative cooling solutions for high-performance compact integrated circuits (ICs).

It is difficult to experimentally measure the properties of nanowires because nonideal factors have much more significant influence on low-dimensional devices as compared with bulk materials, e.g., the large contact resistance between the nanowire and electrodes [11]. Recently, there have been several methods developed to improve the contact resistance, which include etching wires on the substrate; applying epoxy by probe manipulation, using indium pads, and the focused-ion-beam (FIB) method. Li *et al.* [19] and Shi *et al.* [27] used the FIB technique to improve the contact for their nanowire sample and was able to measure the thermal conductance, electrical conductance, and Seebeck coefficient of a single silicon nanowire and carbon nanotube. In this paper, we utilized the thermoreflectance imaging technique to image the heat transfer along the nanowire. Furthermore, we also deducted the thermal conductivity based on the measured heating power and temperature distribution across the nanowire and compared our point measurements with Li *et al.*'s and Shi *et al.*'s resistance measurement.

The thermoreflectance imaging technique is able to provide *in situ* high-resolution images. It is based on temperature dependence of the materials' reflection coefficient. In other words, the temperature change will result in a reflected light intensity change. The normalized change in reflection per unit temperature is defined as the thermoreflectance constant $C_{\rm th}$, which is in the order of 1e-5 for metals. Due to such a small signal, the detected signal is measured with a lock-in amplifier. The thermoreflectance measurement setup is a reliable noncontact temperature-measurement technique, and our system could achieve lateral resolution of 0.5 μm and temperature resolution of 0.1 °C[20]–[22].

II. Experiments

There are many different methods available to synthesis nanowire structures, e.g., thermal evaporation, deep ion etching, electroplating, inorganic electron beam (EB) resistant process [23], and the well-established vapor–liquid–solid (VLS) technique [24]. Our nanowires were grown using the VLS technique. The growth temperature was approximate 800 °C. The size of the nanowires ranges from 5 to 200 nm. The sample under test here was 115-nm wide and 3.9-μm long. The detailed growth mechanism and process control of the experimental sample have been described elsewhere [25], [26].

The microdevice used for external electrical connection for an individual nanowire was fabricated by the standard IC fabrication process [27]. The device consisted of two adjacent 15 μm $\times$ 27 μm low-stress silicon nitride (SiN_x) membranes suspended with five 0.5-μm-thick, 420-μm-long, and 2-μm-wide silicon–nitride beams. A 30-nm-thick and 300-nm-wide platinum thermometer resistance (PTR) coil was deposited on each membrane. The PTR was connected to 200 $\times$ 200 μm Pt bonding pads on the substrate via 1.8-μm-wide Pt leads on the long SiN_x beams. An additional Pt electrode was put on each membrane opposite the other, providing electrical contact for the Si nanowire itself. Fig. 1 illustrates a schematic picture of the microdevice.

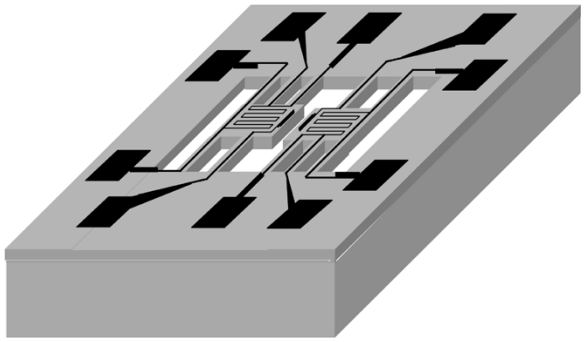

Fig. 1. Schematic picture of microdevice for nanowire electrical connection.

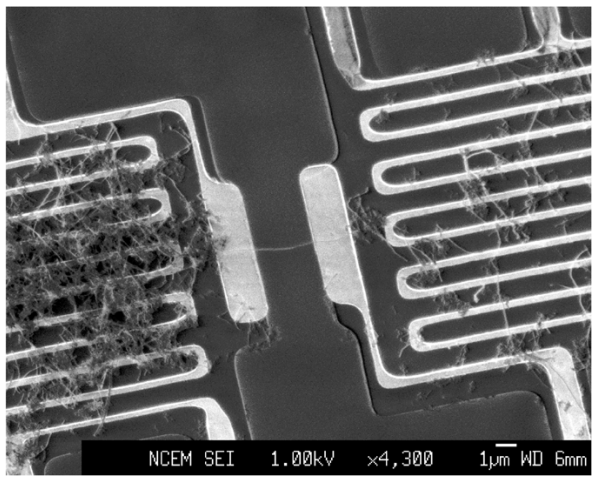

Fig. 2. SEM of a silicon nanowire bridging the two Pt electrodes.

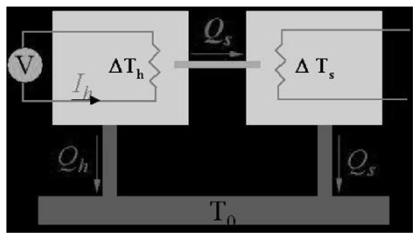

Fig. 3. Silicon nanowire thermal conductivity measurement scheme.

The as-grown Si nanowires were dispersed in an isopronol solution. The nanowire suspension is drop-casted on top of the microdevice and spun to dry. One wire was placed across the bridge between two electrodes. The FIB technique was used to achieve better electrical and thermal contact between the nanowire and electrodes. After all these steps, the sample was ready for the heat-transfer study. Fig. 2 shows a scanning electron micrograph (SEM) image of a silicon nanowire bridging the two Pt electrodes.

To prevent air convection influence on the heat conduction measurements, the sample was put in a cryostat chamber kept in high vacuum from $\sim 10^{-4}$ to 10^{-5} torr with a quartz window. Measurements were then done at room temperature. First, the thermoreflectance coefficient of the sample was calibrated. We put the sample on top of a temperature-controlled stage; when we tune the stage temperature, we could measure the reflected light at the same time. In this way, the $C_{\rm th}$ was calibrated. (8.1 e-5 for current setup) The *I–V* curve of the active PTR was

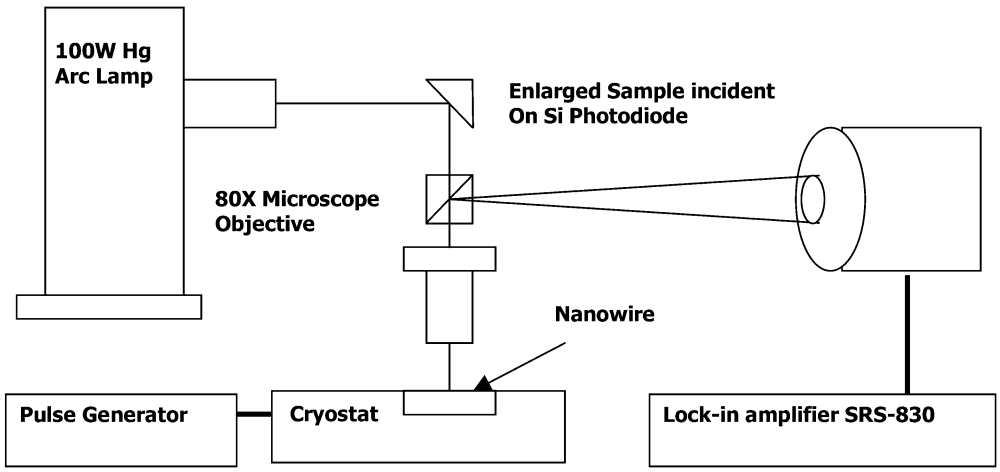

Fig. 4. Schematic setup of thermoreflectance measurement.

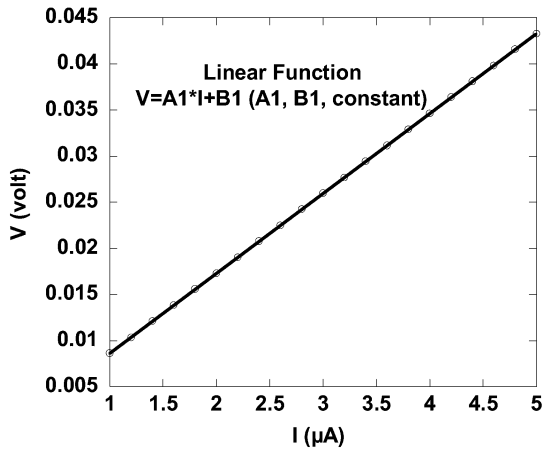

Fig. 5. Nanowire microdevice PRT *I–V* curve with small supplied current. (1–5 μA) under vacuum at room temperature.

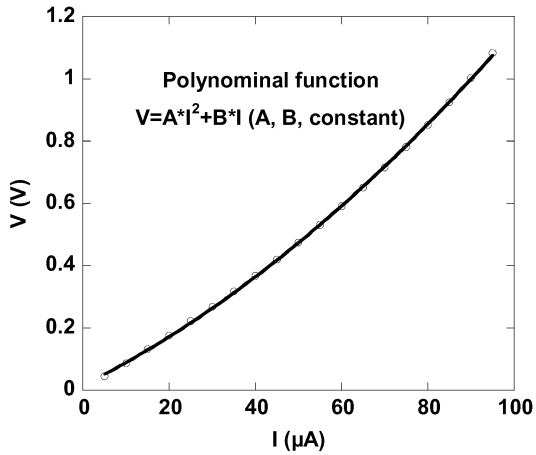

Fig. 6. Nanowire microdevice PRT *I–V* curve with large supplied current. (5–95 μA) under vacuum at room temperature.

then measured with the supplied current range of 1–95 μA, which could be used to calculate the actual power delivered to heat the PTR.

While scanning the temperature profile of the device, a 500-Hz pulsed current with a peak value of 150 μA was delivered to one PTR (active side) and the other PTR was left inactive (inactive side) so that we could create a temperature difference across the Si nanowire, as illustrated in Fig. 3. White light from a 150-W quartz tungsten halogen (QTH) illuminator is focused through an 80$\times$ objective and was reflected back through a beam splitter so that the enlarged image is captured with a photodiode connected to a lock-in amplifier. Fig. 4 demonstrates the thermoreflectance measurement setup.

III. Simulations

In our nanowire device, the dominant time constraint for heat transfer, it is the suspended 0.5-μm SiN_x layer as compared with the 30-nm Pt layer on top of it. To analyze the transient response of the device, we used a three-dimensional (3-D) finite-element thermal model by ANSYS[1] to simulate its transient response and temperature distribution map on the inactive side. In ANSYS, we modeled the SiN_x structure with exactly the same structure

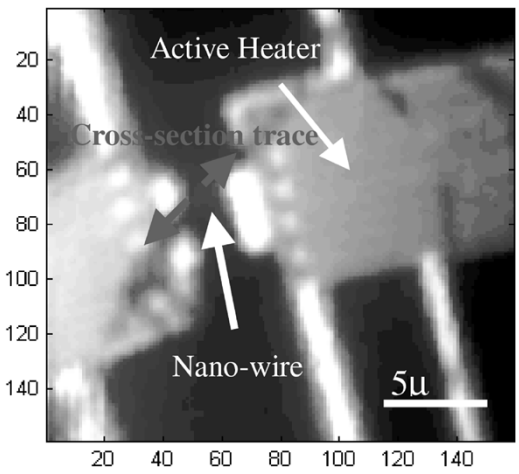

Fig. 7. Normalized thermoreflectance image of silicon nanowire bridging two electrodes and its neighboring PTRs.

as our experimental device. The sample was applied with an adiabatic boundary condition and only the end of the long beam was attached to the heat sink at room temperature. The contact point of the nanowire was set as the heat source with higher temperature, i.e., 40 °C. The 3-D heat conduction equation is solved by the program. The thermal map and transient response

[1]ANSYS Release 7.0, ANSYS Inc., Canonsburg, PA, 2003.

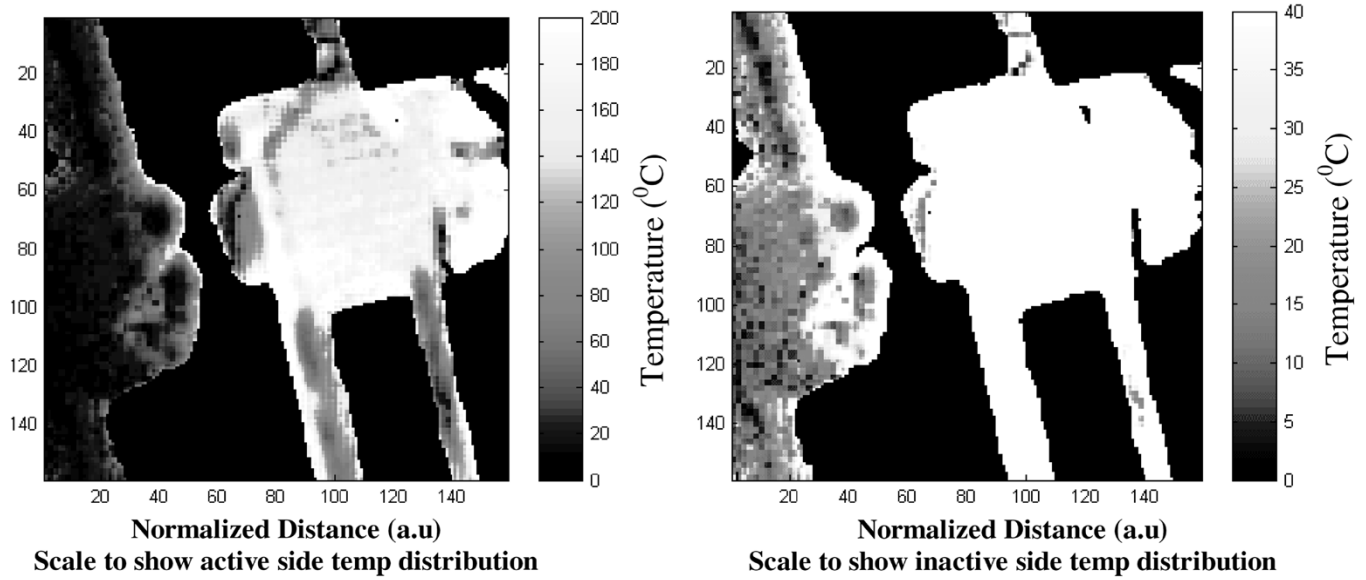

Fig. 8. Thermoreflectance image of temperature contour plot of silicon nanowire device at different temperature scale.

of the device could be estimated, visualized, and compared with thermoreflectance data.

IV. Results and Calculations

Figs. 5 and 6 are the measured *I–V* curves of the active PTR. It was found that, at higher supplied current, the heating temperature was over 100 °C. The nonlinearity of the *I–V* curve in Fig. 6 might due to the temperature coefficient change of the material at high temperature. From Fig. 6, we could find that the voltage across the PTR at any supplied current by the fitted polynomial function of the *I–V* curve. At a supplied current of 150 μA, the voltage across the PTR is 1.96 V. The heating power is thus 295 μW. As illustrated in the measurement scheme in Fig. 4, this power was divided into two parts: heating up the active PTR, defined as Q_{active}, and propagating along the nanowire to heat up the inactive PTR, defined as Q_{inactive}. Since it is in high vacuum condition, we assume that the heat conducted through the nanowire all pass to the inactive PTR side to heat it up. There is no other heat loss. Thus, we could write the equation

$$IV = Q_{\text{active}} + Q_{\text{inactive}}. \tag{1}$$

At the same time, heat power (Q) also has the relation with the PTR thermal conductance (G_l) and its temperature increase (ΔT), which is represented by

$$Q = G_l \Delta T \tag{2}$$

From (1) and (2), we could derive

$$IV = G_l(\Delta T_h + \Delta T_s). \tag{3}$$

(ΔT_h is the temperature increase on the active PTR and ΔT_s is the temperature increase on the inactive PTR.)

We can then calculate the heat conducted through the nanowire by the equation

$$Q_{\text{inactive}} = \frac{\Delta Ts}{(\Delta T_h + \Delta T_s)}(I_h V). \tag{4}$$

Fig. 7 shows the thermoreflectance image of the silicon nanowire bridging two electrodes and its neighboring regions of PTRs. Fig. 8 illustrates the temperature contour plot of the partial region of active and inactive PTRs near the nanowire. It is difficult to get the exact temperature distribution along the silicon nanowire because the width of 100 nm is beyond the resolution of the thermoreflectance technique. The spatial resolution of the thermoreflectance setup is limited by the diffraction limit of the visible light. Furthermore, the nanowire is suspended across the electrodes, which might not be at the same plane as PTRs. It is thus difficult to focus the PTRs and nanowire at the same time. The nanowire appearing in Fig. 8 was believed to actually be the shadow of the nanowire. In Fig. 8, two figures were plotted in different scales to better illustrate the temperature distribution on both the active and inactive sides. Fig. 9 is the phase plot of the thermal image obtained with the lock-in amplifier, indicating the heat flow from the active PTR side to inactive side through the nanowire. Fig. 10 plots the temperature of the electrodes versus the biasing current. From this figure, we could see that with the supplied 150-μA current, the temperature difference across the nanowire is approximately 120 K (160 K on the active side and 40 K on the inactive PTR side). Fig. 11 shows the cross-sectional temperature distribution between two electrodes at 150 μA. The temperature of electrodes plotted in Fig. 10 is the average temperature over the nanowire contact area instead of one point temperature.

The thermal resistance can be defined as

$$R_{\text{th}} = \frac{\Delta T}{Q} \tag{5}$$

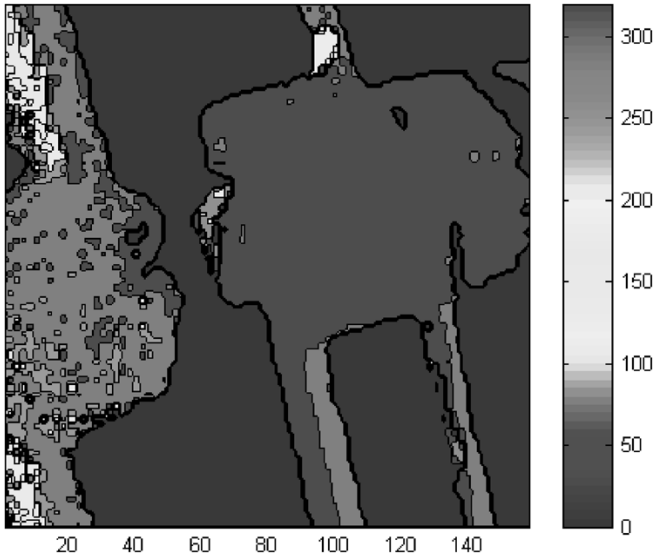

Fig. 9. Themoreflectance image shows silicon nanowire device phase contour plot, suggesting the heat flow across the silicon nanowire.

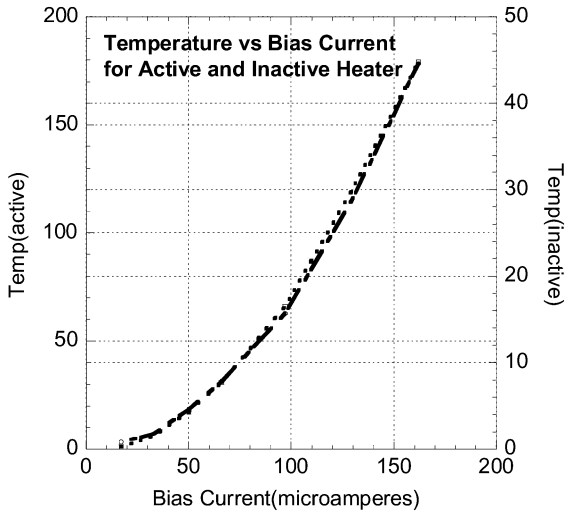

Fig. 10. Nanowire two-end-point (junction points cross electrodes) temperature versus biasing current supplied to the active PTR.

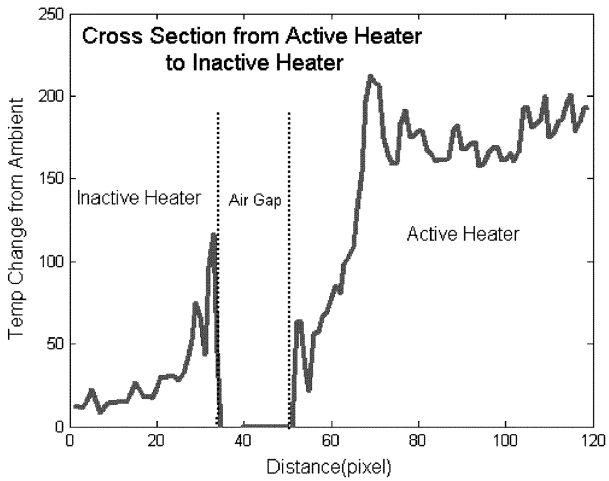

Fig. 11. Cross-sectional temperature distributions.

where ΔT is the temperature difference and Q is the applied heat load. Thus, by combining (5) and (6), the nanowire thermal resistance can be calculated. The thermal resistance of our measured sample is 2.04 e-6 K/W. In addition, the thermal conductivity could be calculated from the following equation:

$$R_{\rm th} = \frac{d}{\beta A} \tag{6}$$

where d is the wire length, A is the wire cross-sectional area, and β is the thermal conductivity. With the known size, the thermal conductivity of 46 W/mK is derived, which corresponds to Li *et al.*'s electrical measurements, i.e., 40 W/mK [19].

The simulation result in Fig. 12 illustrates the temperature map on the inactive PTR side at a different time period. Fig. 13 shows the transient response of the inactive PTR. It takes almost 0.15 s to stabilize the inactive PTR when it is heated up. The experimental frequency was set at 500 Hz to correspond to the measurements done by Li *et al.* at the University of California at Berkeley [27]. Fig. 14 compares the temperature across the device calculated from the 3-D simulation with the thermoreflectance-measured data. It is interesting to find that the temperature exponentially decays as a function of the distance removed from the heat source and the experiments correlates well with the simulation results.

V. Discussion

The thermal conductivity that we obtained using the thermoreflectance technique correlated well with the previous electrical measurement results [27]. In that method, temperature change is based on the measured resistance change of the PTR. Uniform temperature distribution on the membrane surface underneath the PTRs was assumed, thus the temperature of the electrode is equal to the average temperature of the PTR. When one side of the PTR was heated up by the supplied current, the heat propagated along the nanowire also heated the inactive PTR. The resistance change of both the active PTR and inactive PTR was measured and converted to the temperature change from the ambient. Using the electrical measurements method, Li *et al.* measured the thermal conductivity of 40 W/mK at room temperature (300 K). This value is close to what we have calculated here, i.e., 46 W/mK, from thermoreflectance data for the same silicon nanowire sample. The difference between these two techniques is that the thermoreflectance technique directly measured the temperature at the two electrodes where the nanowire bridge cross, instead of the average temperature for the entire membrane surface, by measuring the resistance of the PTR. The 3-D thermal simulation shows the slow transient response of the studied nanowire device due to the suspended SiN_x structure on the order of 0.15 s.

From these experimental results, we found there is indeed a substantial decrease in the thermal conductivity in the nanowire structure as compared with the bulk material. This is an indication that phonons are scattered from the nanowire boundaries. The thermal conductivity could be expressed as

$$\beta_l = \frac{1}{3} C_v v l \tag{7}$$

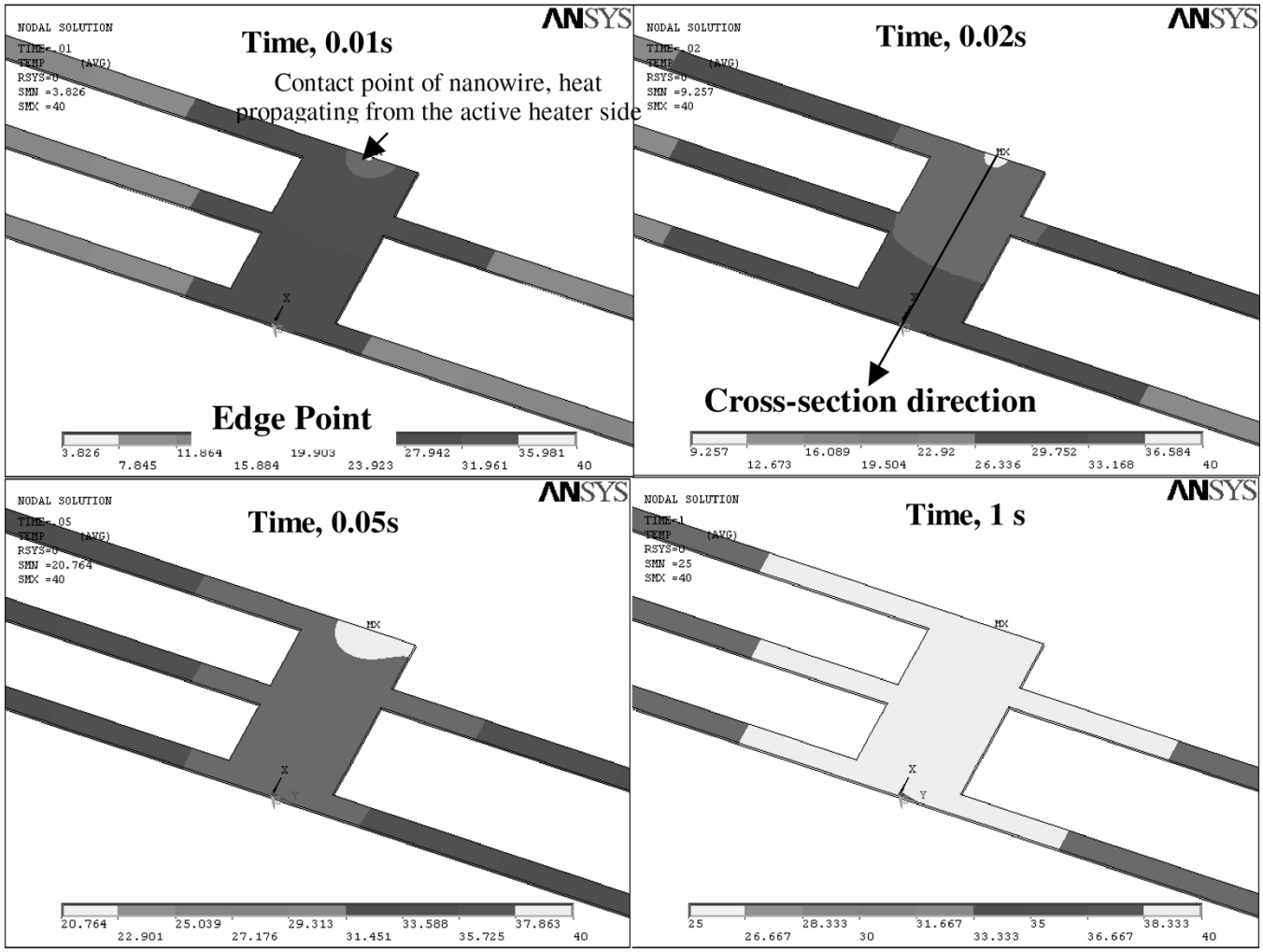

Fig. 12. Simulated temperature distribution of the inactive heater device at different time period.

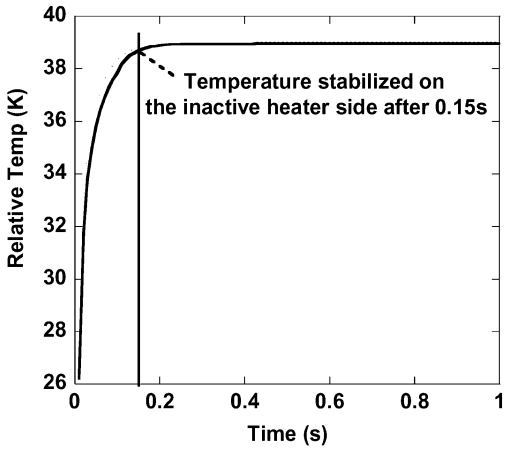

Fig. 13. Transient response of the edge point of inactive PTR side.

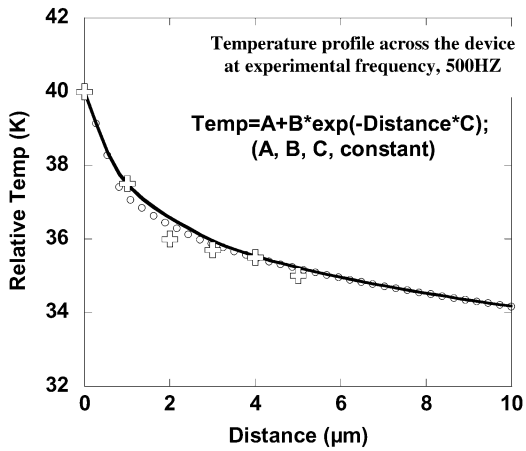

Fig. 14. Temperature profile across the inactive heater direction, as indicated in the thermal map in Fig. 12 at 0.02 s (circles are simulated data, solid line is exponentially fitted curve, crosses are thermoreflectance imaging data).

where C_v is the lattice heat capacity, v is the velocity of the sound in the material, and l is the mean free path. The theory predicted that when the wire width is larger than 200 nm, the thermal conductivity value will be close to the bulk value. The thinner the wire width, the smaller the thermal conductivity. Considering both the reduction of thermal conductivity and possible enhancement of electrical conductivity/carrier mobility through 2-D confinements in the nanowire structure, the figure-of-merit ZT could be significantly improved as compared with bulk silicon.

VI. Future Work

It was believed that the properties of the nanowire was strongly dependent on nanowire size and ambient temperature. Thus, it is necessary to expand current research to other smaller size silicon nanowires and different ambient temperatures. Use of near-field optics could allow thermoreflectance measurement of temperature directly on the nanowire. This could also be used to measure contact thermal resistance between the nanowire and heaters.

References

[1] L. D. Hicks and M. S. Dresselhaus, "Effect of quantum-well structures on the thermoelectric figure of merit," *Phys. Rev. B, Condens. Matter*, vol. 47, no. 19, pp. 12 727–12 731, 1993.

[2] L. D. Hicks and M. S. Dresselhaus, "Thermoelectric figure of merit of a one-dimensional conductor," *Phys. Rev. B, Condens. Matter*, vol. 47, no. 24, pp. 16 631–16 634, 1993.

[3] M. S. Dresslhaus *et al.*, *Recent Trends in Thermoelectric Materials Research III*, T. M. Tritt *et al.*, Eds. San Diego, CA: Academic, 2001.

[4] M. J. Kelly, *Low-Dimensional Semiconductors*. Oxford, U.K.: Clarendon Press, 1995.

[5] A. V. Markel and T. F. George, Eds., *Optics of Nanostructured Materials*. New York: Wiley, 2000.

[6] Y. M. Lin *et al.*, "Theoretical investigation of thermoelectric Bi nanowires," *Phys. Rev. B, Condens. Matter*, vol. 62, pp. 4610–4623, 2000.

[7] T. Koga *et al.*, *Appl. Phys. Lett.*, vol. 73, pp. 2950–2952, 1998.

[8] G. Chen *et al.*, *Thermal Sci. Eng.*, vol. 7, pp. 43–51, 1999.

[9] S. B. Cronin, Y. M. Lin, T. Koga, X. Sun, J. Y. Ying, and M. S. Dresselhaus, "Thermoelectric investigation of bismuth nanowires," in *Proc. 18th Int. Thermoelectrics Conf.*, 1999, pp. 554–557.

[10] W. Wang, W. L. Zhang, L. P. Si, J. Z. Zhang, and J. P. Gao, "Fabrication of thermoelectric materials with bismuth nanowire array," in *Proc. 20th Int. Thermoelectrics Conf.*, 2001, pp. 367–370.

[11] S. B. Cronin, Y. M. Lin, M. R. Black, O. Rabin, and M. S. Dresselhaus, "Thermoelectric transport properties of single bismuth nanowires," in *Proc. 21st Int. Thermoelectronics Conf.*, 2002, pp. 243–248.

[12] M. R. Black, Y. M. Lin, S. B. Cronin, and M. S. Dresslhaus, "Using optical measurements to improve electronic models of bismuth nanowires," in *Proc. 21st Int. Thermoelectronics Conf.*, 2002, pp. 249–252.

[13] Y. M. Lin, X. Sun, and M. S. Dresselhaus, "Theoretical investigation of thermoelectric transport properties of cylindrical Bi nanowires," *Phys. Rev. B, Condens. Matter*, vol. 62, pp. 4610–4623, 2000.

[14] X. Fan, G. Zeng, C. LaBounty, E. Croke, D. Vashaee, A. Shakouri, C. Ahn, and J. E. Bowers, "High cooling power density Si/SiGe microcoolers," *Electron. Lett.*, vol. 37, no. 2, pp. 126–127, Jan. 18, 2001.

[15] X. Fan, G. Zeng, E. Croke, C. LaBounty, C. C. Ahn, A. Shakouri, and J. E. Bowers, "SiGeC/Si superlattice microcoolers," *Appl. Phys. Lett.*, vol. 78, no. 11, pp. 1580–1582, Mar. 12, 2001.

[16] X. Fan, G. Zeng, E. Croke, G. Robinson, C. LaBounty, A. Shakouri, and J. E. Bowers, "SiGe/Si superlattice cooler," *Phys. Low-Dimensional Structures*, no. 5–6, pp. 1–9, 2000.

[17] M. Asen-Palmer *et al.*, "Thermal conductivity of germanium crystals with different isotopic compositions," *Phys. Rev. B, Condens. Matter*, vol. 56, pp. 9431–9447, 1997.

[18] N. Mingo and Y. Liu, "Phonon boundary scattering and the thermal conductivity of crystalline nanowires," presented at the 2nd Semiannual Nanowire Science and Engineering Meeting, Berkeley, CA, Jun. 5, 2002.

[19] D. Li, Y. Wu, P. Kim, L. Shi, P. Yang, and A. Majumdar, "Thermal conductivity of individual silicon nanowires," *Appl. Phys. Lett.*, vol. 83, pp. 2934–2936, 2003.

[20] J. Christofferson, D. Vashaee, A. Shakouri, and P. Melese, "Real time sub-micron thermal imaging using thermoreflectance," presented at the Int. Mechanical Engineering Congr. Exhibit., New York, NY, Nov. 2001.

[21] J. Christofferson, D. Vashaee, A. Shakouri, and P. Melese, "High resolution noncontact thermal characterization of semiconductor devices," *Proc. SPIE*, vol. 4275, pp. 119–125, 2001.

[22] J. Christofferson, D. Vashaee, A. Shakouri, P. Melese, X. Fan, G. Zeng, C. Labounty, J. E. Bowers, and E. T. Croke III, "Thermoreflectance imaging of superlattice micro refrigerator," in *Proc. SEMITHERM XVII Symp.*, San Jose, CA, Mar. 2001, pp. 58–62.

[23] T. Tsutsumi, E. Suzuki, K. Ishii, H. Hiroshima, M. Yamanaka, I. Sakata, and S. Hazra, "Properties of Si nanowire devices fabricated by using an inorganic EB resist process," *Superlattices Microstructures*, vol. 28, no. 5/6, pp. 453–460, 2000.

[24] R. S. Wagner and W. C. Ellis, "Vapor-liquid-solid mechanism of single crystal growth," *Appl. Phys. Lett.*, vol. 4, no. 5, pp. 89–90, 1964.

[25] Y. Wu and P. Yang, "Direct observation of vapor–liquid–solid nanowire growth," *J. Amer. Chem. Soc.*, vol. 123, no. 13, pp. 3165–3168, 2001.

[26] Y. Wu, H. Yan, M. Huang, B. Messer, J. H. Song, and P. Yang, "Inorganic semiconductor nanowires: Rational growth, assembly, and novel properties," *Chem. Eur. J.*, vol. 8, no. 6, pp. 1260–1265, 2002.

[27] L. Shi, D. Li, C. Yu, W. Jang, D. Kim, Z. Yao, P. Kim, and A. Majumdar, "Measuring thermal and thermoelectric properties of one-dimensional nanostructures using a microfabricated device," *J. Heat Transfer*, to be published.

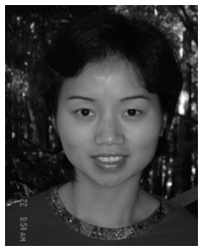

Yan Zhang received the B.S. degree from Shanghai University, Shanghai, China, in 1997, the M.Sc. degree from the National University of Singapore, Singapore, in 2000, and the Ph.D. degree in electrical engineering from the University of California at Santa Cruz, in 2005.

Her current research concerns nanoscale heat and current transport in semiconductor devices, microrefrigerators for on-chip cooling solutions, and thermionic energy conversion for waste heat recovery.

James Christofferson received the B.S. degree in physics, M.S. degree in computer engineering, and Ph.D. degree in electrical engineering from the University of California at Santa Cruz (UCSC), in 1996, 2001, and 2004, respectively. His doctoral dissertation concerned microscale thermal imaging and analysis of semiconductor structures.

He is currently a Post-Doctoral Researcher with the Quantum Electronics Laboratory, UCSC, where he is involved with experiments on optical coherence microscopy and femtosecond pump probe interferometry in order to image phonons and thermal waves and to see beneath opaque surfaces.

Ali Shakouri received the B.S. degree from the Ecole Nationale Superieure des Telecommunications de Paris, Paris, France, in 1990, and the Ph.D. degree from the California Institute of Technology, Pasadena, in 1995.

He is currently an Associate Professor of electrical engineering with the University of California at Santa Cruz. His current research concerns nanoscale heat and current transport in semiconductor devices, submicrometer thermal imaging, microrefrigerators on a chip, and novel optoelectronic ICs. He is the Director of the Thermionic Energy Conversion Center, Santa Cruz, CA, which is a multiuniversity research initiative aimed to improve direct thermal to electric energy conversion technologies.

Dr. Shakouri was the recipient of the 1999 Packard Fellowship and the 2000 National Science Foundation CAREER Award.

Deyu Li received the B.S. degree from the University of Science and Technology of China, Hefei, China, in 1992, the M.E. degree from Tsinghua University, Beijing, China, in 1997, and the Ph.D. degree in mechanical engineering from the University of California at Berkeley, in 2002.

In 2003, he was a Post-Doctoral Researcher with the Mechanical Engineering Department, University of California at Berkeley. In 2004, he joined the Department of Mechanical Engineering, Vanderbilt University, Nashville, TN, as an Assistant Professor. His research interests include microscale/nanoscale thermal and fluid transport phenomena and their engineering applications. Both experimental studies and numerical methods such as molecular dynamics and Monte Carlo simulations are used to explore the nanoscale transport phenomena.

Arun Majumdar received the Ph.D. degree from the University of California at Berkeley, in 1989.

He then served on the mechanical engineering faculties of Arizona State University (1989–1992) and the University of California at Santa Barbara (1992–1996). He currently holds the Almy and Agnes Maynard Chair Professor in Mechanical Engineering with the University of California at Berkeley, where he served as the Vice Chair from 1999 to 2002. His research internists include nanoscale diagnostics, energy conversion and transport in nanostructures, optomechanical microdevices, and nanobiomolecular engineering.

Dr. Majumdar is a member of the Council on Materials Science and Engineering, U.S. Department of Energy, the Chancellor's Advisory Council on Nanoscience and Nanoengineering at the University of California at Berkeley, and the Nanotechnology Technical Advisory Group to the President's Council of Advisors on Science and Technology (PCAST). He is a Fellow of the American Society of Mechanical Engineers (ASME) and the American Association for the Advancement of Science (AAAS). He also serves as chair of the Board of Advisors, American Society of Mechanical Engineers (ASME) Nanotechnology Institute.

Yiying Wu received the B.S. degree in chemical physics from the University of Science and Technology of China, Hefei, China, in 1998, and the Ph.D. degree in chemistry from the University of California at Berkeley, in 2003.

He then performed post-doctoral research with the University of California at Santa Barbara. In Summer 2005, he joined the chemistry faculty of The Ohio State University.

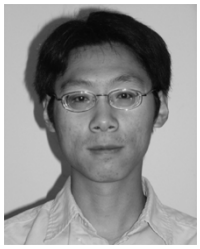

Rong Fan received the B.S. and M.S. degrees in chemistry from the University of Science and Technology of China, Hefei, China, in 1999 and 2001, respectively, and is currently working toward the Ph.D. degree in materials chemistry from the University of California at Berkeley.

His interests include nanostructured semiconductors for thermoelectrics and the fundamentals of inorganic nanotube nanofluidics and their application in single biomolecule sensing and reactions.

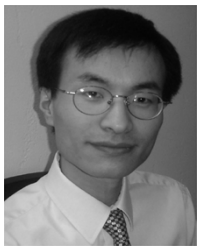

Peidong Yang received the B.S. degree in chemistry from the University of Science and Technology of China, Hefei, China, in 1993, and the Ph.D. degree in chemistry from Harvard University, Cambridge, MA, in 1997.

He then performed post-doctoral research with the University of California at Santa Barbara, prior to joining the faculty of the Department of Chemistry, University of California at Berkeley, in 1999. His main research interest is in the area of 1-D semiconductor nanostructures and their applications in nanophotonics, energy conversion, and nanofluidics.

Dr. Yang was the recipient of the Alfred P. Sloan Research Fellowship, the Arnold and Mabel Beckman Young Investigator Award, the National Science Foundation Young Investigator Award, the Materials Research Society (MRS) Young Investigator Award, the Julius Springer Prize for Applied Physics, and the American Chemical Society (ACS) Pure Chemistry Award.